J. Fluid Mech. (1985), *vol.* 154, *pp.* 253–268
Printed in Great Britain

The hydrodynamic interactions between two spheres in a Brinkman medium

By SANGTAE KIM† AND WILLIAM B. RUSSEL
Department of Chemical Engineering, Princeton University, NJ 08544

(Received 13 September 1983 and in revised form 20 November 1984)

The hydrodynamic interaction between two spheres in a Brinkman medium has been calculated using both the method of reflections and the boundary collocation technique. In particular, calculation of the forces and dipoles for two spheres in a uniform stream and linear field show that the method of reflections converges more rapidly than in the Stokes case, owing to screening of interactions, and that the boundary collocation technique produces accurate solutions at almost all separations (except touching) with relatively few collocation points.

1. Introduction

In this paper we calculate the hydrodynamic interactions between two spheres embedded in a Brinkman medium, i.e. a material characterized by a Newtonian viscosity μ and a permeability α^{-2}, subjected to an ambient velocity field composed of a uniform stream and a linear velocity field. Such solutions are prerequisite to any calculation of the effects of pair interactions on the effective permeability and viscosity of an array of fixed particles. The renormalization techniques presented in the companion paper (Kim & Russel 1985, hereinafter referred to as II) provide one such application. Results are presented for two equal-sized spheres, but may be easily generalized for unequal spheres.

The Brinkman (1947) equation

$$-\nabla p+\mu\nabla^2\boldsymbol{v}-\mu\alpha^2\boldsymbol{v}=\boldsymbol{0} \tag{1.1}$$

for flow through porous media combines the viscous transport of momentum in the Stokes equation

$$-\nabla p+\mu\nabla^2\boldsymbol{v}=\boldsymbol{0} \tag{1.2}$$

with the frictional drag characterized by Darcy's law

$$-\nabla p=\mu\alpha^2\boldsymbol{v}. \tag{1.3}$$

It is used in situations where the pressure-gradient, velocity-gradient and Darcy-resistance terms are all significant (Felderhof 1975; Felderhof & Deutch 1975; Higdon & Kojima 1981; Koplik, Levine & Zee 1983).

Velocity representations for solutions to the Brinkman equation involve scalar functions that are solutions to the Helmholtz equation

$$(\nabla^2-\alpha^2)\psi=0.$$

† Present address: Department of Chemical Engineering and Mathematics Research Center, University of Wisconsin, Madison, WI 53706.

Since this equation is inseparable in bispherical coordinates, this classical technique of low-Reynolds-number hydrodynamics (Stimson & Jeffery 1926; Goldman, Cox & Brenner 1966) cannot be applied to the Brinkman problem. However, we have modified two techniques from low-Reynolds-number flow: the method of reflections and the boundary collocation technique of Gluckman, Pfeffer & Weinbaum (1971). The two complement each other because the collocation technique works even at small (but finite) separations, whereas the method of reflections converges to the desired solution, at a fraction of the computation cost, at large sphere–sphere separations. Furthermore, the method of reflections provides crucial information in the renormalization schemes that are discussed in II.

We discuss the method of reflections in §2, and solve for the uniform stream in §2.1 and linear ambient velocity fields in §§2.2 and 2.3. Section 3 on the boundary collocation solution is divided similarly. The results are presented in the form of dimensionless drag coefficients and stress dipoles (stresslets and torques).

2. The method of reflections

The basic solution strategy is similar to the method of reflections for Stokes flow as given in Happel & Brenner (1965). The original aspect of our work is the development and use of Faxén laws in a Brinkman medium, which greatly facilitate the method.

For two widely separated spheres of radius a with centres at $\boldsymbol{x}_1$ and $\boldsymbol{x}_2$, i.e. $|\boldsymbol{x}_2-\boldsymbol{x}_1| \gg a$, the zeroth-order solution is simply the sum of the solutions for each sphere in isolation, i.e. without hydrodynamic interaction. In our notation these single-sphere solutions are written as $\boldsymbol{v}_1$ and $\boldsymbol{v}_2$. The boundary condition on a sphere is no longer satisfied in this zeroth-order solution, because of the velocity field emanating from the other sphere. Consequently, we augment the solution with two additional velocity fields that cancel the discrepancies at each surface. However, any field that corrects the deviations in the boundary condition at one sphere will upset the matters at the other sphere; hence we get a sequence of velocity fields comprising an iterative approximation.

The method of reflections is so called because the process of creating additional velocity fields to match the boundary conditions can be visualized as reflections from an incident field. The schematic diagram of the reflection process (figure 1) shows that a reflected field becomes an incident field on the other surface at the next reflection. We will use the following convention for labelling the velocity fields. If the reflection occurs at the sphere at $\boldsymbol{x}_\beta$ we label the reflected field by adding the subscript β ($\beta = 1, 2$) to the subscripts for the incident field. Note that the isolated single-sphere solutions may be considered as reflections from the ambient velocity field $\boldsymbol{v}^\infty$. We will call this the zeroth reflection, in accord with the literature. The fields reflected from the single-sphere solutions are the first reflections, and those from an nth reflection field are referred to as $(n+1)$th reflection fields.

Given an incident field, we need a method for calculating the reflected field. Happel & Brenner (1965) use Lamb's general solution with Hobson's (1955) addition theorems for transforming the spherical harmonic from a coordinate system centred at one sphere to one centred at the other. A similar approach may be used for the Brinkman equation, using the velocity representation in Stratton (1941) and the addition theorem presented in Glendinning & Russel (1983), but the algebraic manipulations are cumbersome. Instead, we present an approach based on Faxén laws and the integral representation for the Brinkman equation. Our technique has the

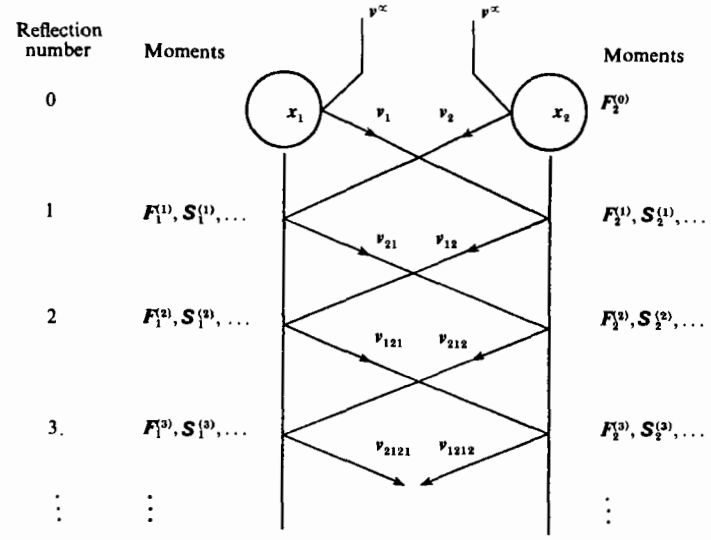

FIGURE 1. A schematic representation of the reflection procedure.

advantage of directly producing the quantities of interest – the force, torque and stresslet on the spheres.

As discussed by Howells (1974), the incident field $\boldsymbol{v}^{\mathrm{I}}(\boldsymbol{x})$ can be cancelled at the sphere surface (for the sphere centred at $\boldsymbol{x}_1$) by a reflection field having the following integral representation:

$$v_i(\boldsymbol{x}) = \frac{-1}{8\pi\mu}\int_{S_P} (\boldsymbol{\sigma}\cdot\boldsymbol{n})_j \mathscr{J}_{ij}(\boldsymbol{x}-\boldsymbol{x}';\alpha)\,\mathrm{d}A$$

$$= \frac{-1}{8\pi\mu}\sum_{n=0}^{\infty}\frac{(-1)^n}{n!}\left[\int_{S_P}(\boldsymbol{\sigma}\cdot\boldsymbol{n})_j\, x'_{k_1}x'_{k_2}\ldots x'_{k_n}\,\mathrm{d}A\right]\mathscr{J}_{ij,k_1\ldots k_n}(\boldsymbol{x}-\boldsymbol{x}_1;\alpha), \quad (2.1)$$

where $\boldsymbol{\sigma}$ is the stress evaluated at the surface, $\boldsymbol{x}'$ is a vector from the centre to a point on the surface, and $\mathscr{J}$ is the Green dyadic given by

$$\mathscr{J}(\boldsymbol{x};\alpha) = \boldsymbol{\delta}\frac{2}{\alpha^2 r^3}[(1+\alpha r+\alpha^2 r^2)\,\mathrm{e}^{-\alpha r}-1]+\boldsymbol{xx}\frac{6}{\alpha^2 r^5}[1-(1+\alpha r+\tfrac{1}{3}\alpha^2 r^2)\,\mathrm{e}^{-\alpha r}]. \quad (2.2)$$

Once the multipole moments, $\int_S(\boldsymbol{\sigma}\cdot\boldsymbol{n})\,\boldsymbol{x}'\boldsymbol{x}'\ldots\boldsymbol{x}'\,\mathrm{d}S$ in (2.1) are related to $\boldsymbol{v}^{\mathrm{I}}$, the solution scheme can proceed by calculating each reflection to the desired accuracy. Such relations, known as the Faxén (1922, 1927) laws, may be derived for the Brinkman equation by generalizing a procedure first suggested by Howells (1974). He derived the Faxén law for the force (monopole moment) by applying the operator $\{B_0(\alpha a)+B_2(\alpha a)\,a^2\nabla^2\}$, with $B_0(x) = 1+x+\frac{1}{3}x^2$ and $B_2(x) = (\mathrm{e}^x-B_0)/x^2$, to the integral representation for flow past a sphere centred at $\boldsymbol{x}_1$:

$$\boldsymbol{v}(\boldsymbol{x}) = \boldsymbol{v}^{\mathrm{I}}(\boldsymbol{x})-\frac{1}{8\pi\mu}\int_{S_P}(\boldsymbol{\sigma}\cdot\boldsymbol{n})_j\,\mathscr{J}_{ij}(\boldsymbol{x}-\boldsymbol{x}';\alpha)\,\mathrm{d}A. \quad (2.3)$$

Since $\boldsymbol{v}(\boldsymbol{x})$ and its gradients vanish inside the sphere, and since

$$\{B_0(\alpha a)+B_2(\alpha a)\,a^2\nabla^2\}\mathscr{J}(\boldsymbol{x}-\boldsymbol{x}';\alpha)|_{\boldsymbol{x}-\boldsymbol{x}_1} = \frac{4}{3a}\boldsymbol{\delta}, \quad (2.4)$$

the result is

$$\boldsymbol{F} = \int_{S_P} \boldsymbol{\sigma}\cdot\boldsymbol{n}\,\mathrm{d}A = 6\pi\mu a\{B_0(\alpha a) + B_2(\alpha a)\, a^2\nabla^2\}\, \boldsymbol{v}^{\mathrm{I}}(\boldsymbol{x})|_{x=x_1}. \tag{2.5}$$

Howells also gives the force due to the pressure alone as

$$\boldsymbol{F}_p = \int_{S_P} (\boldsymbol{\sigma}\cdot\boldsymbol{n})\cdot\boldsymbol{nn}\,\mathrm{d}A = 2\pi\mu a\{P_0(\alpha a) + P_2(\alpha a)\, a^2\nabla^2\}\, \boldsymbol{v}^{\mathrm{I}}(\boldsymbol{x})|_{x=x_1},$$

with $$P_0(x) = 1+x+x^2, \quad P_2(x) = \frac{\mathrm{e}^x - P_0}{x^2}.$$

This procedure may be repeated with operators involving higher-order derivatives. The key point is that they should generate the polyadic

$$\boldsymbol{\delta x' x' \ldots x'},$$

when applied to the Green dyadic, in order that the surface integral in (2.1) reduce to the appropriate multipole moment. The Faxén laws for the dipole moment, decomposed into the symmetric (stresslet $\boldsymbol{S}$) and antisymmetric (couplet $\boldsymbol{T}$) parts, are

$$\frac{1}{2}\int_{S_P} [(\boldsymbol{\sigma}\cdot\boldsymbol{n})\,\boldsymbol{x}' + \boldsymbol{x}'(\boldsymbol{\sigma}\cdot\boldsymbol{n})]\,\mathrm{d}A = \frac{1}{3}\int_{S_P} \boldsymbol{\sigma}:\boldsymbol{nn}\,\mathrm{d}A\,\boldsymbol{\delta} + \tfrac{20}{3}\pi\mu a^3\{C_0(\alpha a) + C_2(\alpha a)\, a^2\nabla^2\}\,\boldsymbol{e}^{\mathrm{I}}|_{x=x_1}, \tag{2.6}$$

$$\frac{1}{2}\int_{S_P} [(\boldsymbol{\sigma}\cdot\boldsymbol{n})\,\boldsymbol{x}' - \boldsymbol{x}'(\boldsymbol{\sigma}\cdot\boldsymbol{n})]\,\mathrm{d}A = -\frac{4\pi\mu a^3\,\mathrm{e}^{\alpha a}}{1+\alpha a}\,\tfrac{1}{2}(\nabla\boldsymbol{v}^{\mathrm{I}} - \nabla\boldsymbol{v}^{\mathrm{IT}})|_{x=x_1}, \tag{2.7}$$

with the rate-of-strain tensor defined as $\boldsymbol{e} = \frac{1}{2}(\nabla\boldsymbol{v} + \nabla\boldsymbol{v}^{\mathrm{T}})$,

$$C_0(x) = \frac{1 + x + \frac{2}{5}x^2 + \frac{1}{15}x^3}{1+x} \tag{2.7a}$$

and

$$C_2(x) = \frac{\mathrm{e}^x - (1+x)\,C_0}{x^2(1+x)}. \tag{2.7b}$$

Similarly, it can be shown that for the quadrupoles

$$\begin{aligned}(\boldsymbol{Q}\cdot\nabla):\nabla\mathscr{J} &= \left\{\left[\int_{S_P} (\boldsymbol{\sigma}\cdot\boldsymbol{n})\,\boldsymbol{x}'\boldsymbol{x}'\,\mathrm{d}A\right]\cdot\nabla\right\}:\nabla\mathscr{J} \\ &= \frac{a^2}{4}\,\boldsymbol{F}_p\cdot\nabla^2\mathscr{J} + \frac{a^2[1+\alpha a - \frac{1}{15}(\alpha a)^2]}{4B_0(\alpha a)}\,\boldsymbol{F}\cdot\nabla^2\mathscr{J}.\end{aligned}$$

These relations suffice for our purposes. Higher-order relations are necessary, however, in any drag calculations requiring accuracy beyond that provided by four reflections.

2.1. *The drag on two spheres in a uniform stream*

In this subsection we will calculate the drag on the sphere at $\boldsymbol{x}_1$, including the contribution from the hydrodynamic interaction with the sphere centred at $\boldsymbol{x}_2$, by the method of reflections. The leading-order term is the contribution from the zeroth reflection, i.e. the single-sphere result given by Brinkman (1947):

$$\boldsymbol{F}_1^{(0)} = 6\pi\mu a B_0(\alpha a)\,\boldsymbol{U},$$

where $\boldsymbol{U}$ is the uniform velocity. The velocity field generated by this reflection is the single-sphere solution

$$\boldsymbol{v}_1 = -\boldsymbol{F}_1^{(0)}\cdot\left\{1+\frac{B_2}{B_0}\,a^2\nabla^2\right\}\mathscr{J}(\boldsymbol{x}-\boldsymbol{x}_1;\,\alpha)/8\pi\mu. \tag{2.8}$$

The velocity field $\boldsymbol{v}_2$ is obtained by switching the subscripts. These solutions are equivalent to those given by Brinkman (1947) and Howells (1974), but are in a form that is more useful for multi-particle interaction problems.

The first correction comes from the disturbance due to the Brinkman solution $\boldsymbol{v}_2$ from the sphere at $\boldsymbol{x}_2$. The first reflection at $\boldsymbol{x}_1$ cancels this disturbance with the reflected field $\boldsymbol{v}_{21}$. We represent this velocity field to leading order in inverse separation with monopoles, dipoles and degenerate quadrupoles with strengths given by the Faxén laws as

$$\begin{aligned}\boldsymbol{F}_1^{(1)} &= 6\pi\mu a\{B_0+B_2a^2\nabla^2\}\,\boldsymbol{v}_2(\boldsymbol{x})\,|_{x=x_1}\\ &= -6\pi\mu a\boldsymbol{U}\cdot\tfrac{3}{4}a\{B_0^2+[2B_0B_2+(\alpha a)^2B_2^2]\,a^2\nabla^2\}\,\mathscr{J}(\boldsymbol{x}-\boldsymbol{x}_2;\,\alpha)\,|_{x=x_1}.\end{aligned} \tag{2.9}$$

We have used $\nabla^4\mathscr{J} = \alpha^2\nabla^2\mathscr{J}$ in (2.9). The dipoles are given by the Faxén laws with $\boldsymbol{v}^{\mathrm{I}}$ replaced by $\boldsymbol{v}_2$:

$$\boldsymbol{S}_1^{(1)} = \tfrac{20}{3}\pi\mu a^3\{C_0(\alpha a)+C_2(\alpha a)\,a^2\nabla^2\}\,\boldsymbol{e}_2\,|_{x=x_1}, \tag{2.10}$$

$$\boldsymbol{T}_1^{(1)} = -\frac{4\pi\mu a^3\,\mathrm{e}^{\alpha a}}{1+\alpha a}\,\tfrac{1}{2}(\nabla\boldsymbol{v}_2-\nabla\boldsymbol{v}_2^{\mathrm{T}})\,|_{x=x_1}, \tag{2.11}$$

$$(\boldsymbol{Q}\cdot\nabla):\nabla\mathscr{J} = \frac{a^2}{4}\,\boldsymbol{F}_p^{(1)}\cdot\nabla^2\mathscr{J}+\frac{a^2[1+\alpha a-\frac{1}{15}(\alpha a)^2]}{4B_0(\alpha a)}\,\boldsymbol{F}_1^{(1)}\cdot\nabla^2\mathscr{J}. \tag{2.12}$$

The multipole expansion for $\boldsymbol{v}_{21}$ is

$$\boldsymbol{v}_{21} = -\boldsymbol{F}_1^{(1)}\cdot\left\{1+\frac{B_2}{B_0}\,a^2\nabla^2\right\}\mathscr{J}(\boldsymbol{x}-\boldsymbol{x}_1;\,\alpha)/8\pi\mu+(\boldsymbol{S}_1^{(1)}+\boldsymbol{T}_1^{(1)}):\nabla\mathscr{J}(\boldsymbol{x}-\boldsymbol{x}_1;\,\alpha)/8\pi\mu+\ldots. \tag{2.13}$$

The multipole expansion for $\boldsymbol{v}_{12}(\boldsymbol{x})$, obtained by switching indices 1 and 2 in (2.13), leads to the second reflection contribution to the drag:

$$\boldsymbol{F}_1^{(2)} = 6\pi\mu a\{B_0(\alpha a)+B_2(\alpha a)\,a^2\nabla^2\}\,\boldsymbol{v}_{12}(\boldsymbol{x})\,|_{x=x_1}. \tag{2.14}$$

The leading-order terms in the third and fourth reflection contributions to the drag are obtained by keeping only the monopole terms in each reflection:

$$\boldsymbol{F}_1^{(3)} = 6\pi\mu a[-\tfrac{3}{4}aB_0]^3\,\boldsymbol{U}\cdot\mathscr{J}^3(\boldsymbol{x}_2-\boldsymbol{x}_1), \tag{2.15}$$

$$\boldsymbol{F}_1^{(4)} = 6\pi\mu a[-\tfrac{3}{4}aB_0]^4\,\boldsymbol{U}\cdot\mathscr{J}^4(\boldsymbol{x}_1-\boldsymbol{x}_2). \tag{2.16}$$

The drag on sphere 1 is the sum of these contributions:

$$\boldsymbol{F}_1 = \boldsymbol{F}_1^{(0)}+\boldsymbol{F}_1^{(1)}+\boldsymbol{F}_1^{(2)}+\boldsymbol{F}_1^{(3)}+\boldsymbol{F}_1^{(4)}+\ldots. \tag{2.17}$$

The contributions to the drag from each reflection can be decomposed into components parallel and perpendicular to the sphere–sphere axis $\boldsymbol{R}$. Thus the final result may be expressed as

$$\boldsymbol{F} = 6\pi\mu aB_0\,\boldsymbol{U}\cdot[X_F(R;\,\alpha)\,\boldsymbol{RR}+Y_F(R;\,\alpha)\,(\boldsymbol{\delta}-\boldsymbol{RR})], \tag{2.18}$$

Results for X_F and Y_F are shown in figures 4 and 5 for $\alpha a = 0.1$, 1.0 and 10.0. The collocation results are also shown in these figures. A comparison of the two methods is deferred to §4.

2.2. *The stresslet on two spheres in a rate-of-strain field*

The stresslet or dipole induced in a sphere in a constant rate-of-strain field $\boldsymbol{E}$ enters into the calculation of the particle contribution to the bulk stress. The calculations for force-free particles (spheres) in situations governed by the Stokes equations are available in Batchelor & Green (1972). In paper II we encountered analogous problems in the Brinkman medium, since momentum transfer due to velocity gradients can be significant in moderately permeable porous media.

The relevant boundary-value problem is as follows. Two stationary spheres with centres at $\boldsymbol{x}_1$ and $\boldsymbol{x}_2$ are placed in an ambient linear field $\boldsymbol{v}^\infty = \boldsymbol{E}\cdot(\boldsymbol{x}-\boldsymbol{x}_1)$. The spheres are not force-free, because they are fixed and do not flow with the fluid. We now use the method of reflections to calculate the stresslet on the sphere at $\boldsymbol{x}_1$.

The leading-order contributions from the zeroth reflection, i.e. the single-sphere stresslet and the velocity fields at each sphere, are

$$\boldsymbol{S}_1^{(0)} = \tfrac{20}{3}\pi\mu a^3 C_0(\alpha a)\,\boldsymbol{E}, \tag{2.19}$$

$$\boldsymbol{v}_1 = \tfrac{20}{3}\pi\mu a^3(\boldsymbol{E}\cdot\boldsymbol{\nabla})\cdot\{C_0 + C_2\,a^2\nabla^2\}\,\boldsymbol{\mathcal{J}}(\boldsymbol{x}-\boldsymbol{x}_1)/8\pi\mu, \tag{2.20}$$

$$\boldsymbol{v}_2 = 6\pi\mu a[\boldsymbol{E}\cdot(\boldsymbol{x}_2-\boldsymbol{x}_1)]\cdot\{B_0 + B_2\,a^2\nabla^2\}\,\boldsymbol{\mathcal{J}}(\boldsymbol{x}-\boldsymbol{x}_2)/8\pi\mu. \tag{2.21}$$

Thus $\boldsymbol{v}_1$ is composed of Brinkman dipole and octupole fields in a linear field centred at $\boldsymbol{x}_1$, while $\boldsymbol{v}_2$, to leading order, is the monopole field generated by the sphere at $\boldsymbol{x}_2$ in a uniform stream of strength $\boldsymbol{E}\cdot(\boldsymbol{x}_2-\boldsymbol{x}_1)$. By following the pattern discussed in §2.1, the higher-order contributions to the stresslet at $\boldsymbol{x}_1$ are determined as

$\tfrac{20}{3}\pi\mu a^3\{C_0 + C_2\,a^2\nabla^2\}$ operating on the rate-of-strain fields:

$$\begin{aligned}
&-\tfrac{3}{4}a(B_0 + B_2\,a^2\nabla^2)\,(\boldsymbol{E}\cdot(\boldsymbol{x}_2-\boldsymbol{x}_1))\cdot\boldsymbol{\mathcal{J}}(\boldsymbol{x}-\boldsymbol{x}_2) + \tfrac{5}{6}a^3(C_0 + C_2\,a^2\nabla^2)\,\boldsymbol{E}:\boldsymbol{\nabla}\boldsymbol{\mathcal{J}}(\boldsymbol{x}-\boldsymbol{x}_2)\\
&-\tfrac{3}{4}a(B_0 + B_2\,a^2\nabla^2)\,\tfrac{5}{6}a^3(C_0 + C_2\,a^2\nabla^2)\,\boldsymbol{E}:\boldsymbol{\nabla}\boldsymbol{\mathcal{J}}(\boldsymbol{x}_2-\boldsymbol{x}_1)\cdot\boldsymbol{\mathcal{J}}(\boldsymbol{x}-\boldsymbol{x}_2)\\
&+(-\tfrac{3}{4}aB_0)^3\,(\boldsymbol{E}\cdot(\boldsymbol{x}_2-\boldsymbol{x}_1))\cdot\boldsymbol{\mathcal{J}}\cdot\boldsymbol{\mathcal{J}}\cdot\boldsymbol{\mathcal{J}}(\boldsymbol{x}-\boldsymbol{x}_2).
\end{aligned} \tag{2.22}$$

The three lines correspond to the first, second and third reflections in that order.

The terms in (2.22) can be rearranged into the canonical form associated with the symmetry about the sphere–sphere axis $\boldsymbol{R}$. As shown by Brenner (1972), the linear relation between the stresslet and the ambient rate of strain requires only three independent scalar functions. Thus

$$\begin{aligned}
S_{ij} = \tfrac{20}{3}\pi\mu a^3 C_0\,E_{kl}\{&\tfrac{3}{2}X_S(R_i R_j - \tfrac{1}{3}\delta_{ij})\,(R_k R_l - \tfrac{1}{3}\delta_{kl})\\
&+\tfrac{1}{2}Y_S(R_i\delta_{jl}R_k + R_j\delta_{il}R_k + R_i\delta_{jk}R_l + R_j\delta_{ik}R_l - 4R_i R_j R_k R_l)\\
&+\tfrac{1}{2}Z_S(\delta_{ik}\delta_{jl} + \delta_{jk}\delta_{il} - \delta_{ij}\delta_{kl} + R_i R_j\delta_{kl} + \delta_{ij}R_k R_l\\
&-R_i\delta_{jl}R_k - R_j\delta_{il}R_k - R_i\delta_{jk}R_l - R_j\delta_{ik}R_l + R_i R_j R_k R_l)\}.
\end{aligned} \tag{2.23}$$

This expression is structured so that the X_S, Y_S and Z_S functions are associated with the following canonical flows: axisymmetric extensional flow, hyperbolic straining in a plane containing the sphere–sphere axis, and hyperbolic straining in a plane perpendicular to the sphere–sphere axis. The results for X_S, Y_S and Z_S are plotted in figures 6–8 for $\alpha a = 0.1$, 1.0 and 10.0. A discussion of the comparison with the collocation results is deferred to §4.

2.3. *The torque on two spheres in a vorticity field*

The torque induced by the ambient field $\boldsymbol{\Omega}^{\mathrm{T}}\cdot(\boldsymbol{x}-\boldsymbol{x}_1)$ can be calculated along the lines shown in the preceding discussion. The contributions from the reflections follow:

$$\boldsymbol{T}_1^{(0)} = -\frac{4\pi\mu a^3\,\mathrm{e}^{\alpha a}}{1+\alpha a}\,\boldsymbol{\Omega}, \tag{2.24}$$

$$\boldsymbol{T}_{1ij}^{(1)} = \frac{4\pi\mu a^3\,\mathrm{e}^{\alpha a}}{1+\alpha a}\,\tfrac{3}{4}a[\boldsymbol{\Omega}^{\mathrm{T}}\cdot(\boldsymbol{x}_2-\boldsymbol{x}_1)]_k\{B_0+B_2a^2\nabla^2\}\tfrac{1}{2}(\mathscr{J}_{jk,i}-\mathscr{J}_{ik,j})|_{x=x_1}$$
$$+\frac{4\pi\mu a^3\,\mathrm{e}^{\alpha a}}{1+\alpha a}\,\frac{a^3}{2}\,\frac{\mathrm{e}^{\alpha a}}{1+\alpha a}\,\Omega_{kl}\tfrac{1}{2}(\mathscr{J}_{jk,li}-\mathscr{J}_{ik,lj})|_{x=x_1}, \tag{2.25}$$

$$\boldsymbol{T}_{1ij}^{(2)} = \frac{4\pi\mu a^3\,\mathrm{e}^{\alpha a}}{1+\alpha a}\,\tfrac{3}{4}av_{1k}\{B_0+B_2a^2\nabla^2\}\tfrac{1}{2}(\mathscr{J}_{jk,i}-\mathscr{J}_{ik,j})|_{x=x_1}, \tag{2.26}$$

with
$$v_1 = \frac{a^3}{2}\,\frac{\mathrm{e}^{\alpha a}}{1+\alpha a}\,\boldsymbol{\Omega}:\nabla\mathscr{J}(\boldsymbol{x}-\boldsymbol{x}_1)|_{x=x_2},$$

$$\boldsymbol{T}_{1ij}^{(3)} = \frac{4\pi\mu a^3\,\mathrm{e}^{\alpha a}}{1+\alpha a}\,\tfrac{3}{4}aB_0\{[\boldsymbol{\Omega}^{\mathrm{T}}\cdot(\boldsymbol{x}_2-\boldsymbol{x}_1)]\cdot\mathscr{J}^2\}_k\tfrac{1}{2}(\mathscr{J}_{jk,i}-\mathscr{J}_{ik,j})|_{x=x_1}. \tag{2.27}$$

The two-sphere symmetry permits the decomposition of the associated pseudo-vectors into components parallel and perpendicular to the sphere–sphere axis $\boldsymbol{R}$. The contributions from the reflections are collected as

$$\boldsymbol{T} = 8\pi\mu a^3\boldsymbol{\Omega}\cdot[X_T(R;\alpha)\,\boldsymbol{RR}+Y_T(R;\alpha)\,(\boldsymbol{\delta}-\boldsymbol{RR})], \tag{2.28}$$

with $T_i = -\epsilon_{ijk}T_{jk}$ and $\Omega_i = \frac{1}{2}\epsilon_{ijk}\Omega_{jk}$. The results are plotted in figures 9 and 10 for $\alpha a = 0.1$, 1.0 and 10.0.

3. The boundary collocation solution

The method of reflections converges slowly when the two spheres are close together. Since the algebraic manipulations become increasingly complicated for the higher-order terms, another approach must be considered. The boundary collocation technique developed by Gluckman *et al.* (1971) accurately solves the near-field problem. The two techniques give identical results in the far-field, as shown in figures 4–10, but the method of reflections was used where possible, since it required less computer time. Together these two techniques provided the complete solution of the two-sphere problem at all separations.

We construct our collocation solution in such a way that we obtain the entire collection of hydrodynamic functions X_F, Y_F, X_S, Y_S, Z_S, X_T and Y_T from a 'master solution'. We do this by noting that all ambient velocities of interest are contained in the following general expression for the boundary condition on the disturbance velocity. On the surface of sphere 1 we write

$$\boldsymbol{v}_s = -\boldsymbol{v}^{\infty} = \sum_{l=1}^{2}\sum_{m=0}^{l}[\nabla\{r_1^l P_l^m(\cos\theta_1)\,[A_{l0}\,\delta_{0m}+A_{lm}\sin m\phi]\}$$
$$+\nabla\times\{r_1\,r_1^l P_l^m(\cos\theta_1)\,B_{lm}\cos m\phi\}]. \tag{3.1}$$

The spherical coordinates (r_1,θ_1,ϕ) have their origin at $\boldsymbol{x}_1$, and the z-axis points from

	Non-zero coefficient	v_s	Hydrodynamic function(s)
(1)	$A_{10} = 1$	uniform stream parallel to sphere–sphere axis	X_F
(2)	$A_{11} = 1$	uniform stream perpendicular to axis	Y_F
(3)	$A_{20} = 1$	axisymmetric straining	X_S
(4)	$A_{21} = 1$	rate of strain as in (Z, X)-shear flow	Y_S
(5)	$A_{22} = 1$	hyperbolic straining in (X, Y)-plane	Z_S
(6)	$B_{10} = 1$	vorticity parallel to sphere–sphere axis	X_T
(7)	$B_{11} = 1$	vorticity perpendicular to sphere–sphere axis	Y_T

TABLE 1

sphere 2 to sphere 1. The reason for the particular form for the ϕ-dependence in (3.1) will become apparent later on, when we examine the velocity components. In table 1 we show how the various ambient fields are constructed.

We now present the velocity representation and discuss the key idea behind the solution technique. Following Ganatos, Pfeffer & Weinbaum (1978), the velocity is written as a superposition of two expansions, one centred at sphere 1 and the other centred at sphere 2. In figure 2, θ_2 is defined as the complement of the conventional polar angle to eliminate a factor of $(-1)^n$ in the subsequent analysis. Ganatos *et al.* (1978) used Lamb's general solution for the Stokes equation. For the Brinkman equation we can use the following representation from Stratton (1941) for each expansion:

$$-\frac{1}{\mu\alpha^2}\nabla p + \nabla\times\nabla\times(x\Phi) + \nabla\times(x\chi), \tag{3.2}$$

with the pressure field p, poloidal field Φ and toroidal field χ satisfying

$$\nabla^2 p = 0, \quad \nabla^2\Phi - \alpha^2\Phi = 0, \quad \nabla^2\chi - \alpha^2\chi = 0. \tag{3.3a,b,c}$$

Separation of variables in spherical coordinates gives

$$p = \sum_{n=1}^{\infty}\sum_{m=0}^{n} a_{mn}\, r^{-n-1}\, P_n^m(\cos\theta)\,(\delta_{0m} + \sin m\phi), \tag{3.4a}$$

$$\Phi = \sum_{n=1}^{\infty}\sum_{m=0}^{n} b_{mn}\, k_n(\alpha r)\, P_n^m(\cos\theta)\,(\delta_{0m} + \sin m\phi), \tag{3.4b}$$

$$\chi = \sum_{n=1}^{\infty}\sum_{m=0}^{n} c_{mn}\, k_n(\alpha r)\, P_n^m(\cos\theta)\cos m\phi. \tag{3.4c}$$

The modified spherical Bessel function k_n is defined as in Abramowitz & Stegun (1965).

The collocation technique finds approximate values for the coefficients a_{mn}, b_{mn} and c_{mn} by truncating the series at $n = N$ and satisfying the boundary conditions at N collocation points on each sphere. We will show shortly that each problem requires only one particular value for m, so that in the general case we have $6N$ unknowns and $6N$ equations ($2N$ collocation points times 3 velocity components). The success of the collocation technique is due to the rapid convergence with respect to increasing N.

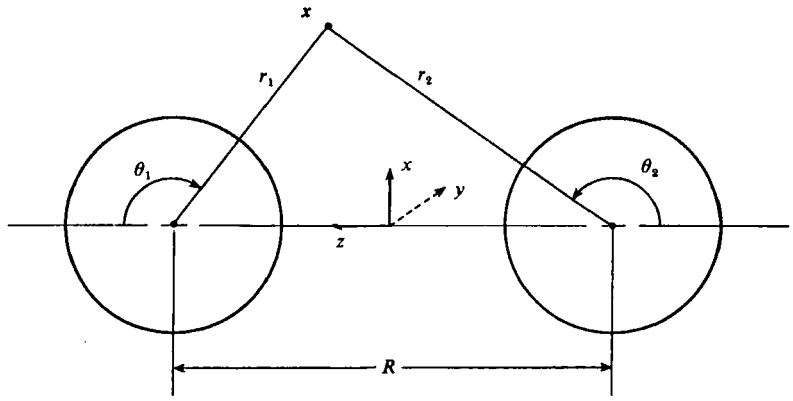

FIGURE 2. The two-sphere geometry.

We now take advantage of the two-sphere symmetry to simplify the problem. First, the problem can be reduced to a one-dimensional collocation in θ, even if the flow is not axisymmetric. This simplification was missed by Ganatos *et al.* (1978) but was exploited in a later work (Ganatos, Pfeffer & Weinbaum 1980). Secondly, for flows with symmetry about the (X, Y)-plane, the coefficients for the expansion at sphere 2 either equal or are negatives of the corresponding coefficient in the other expansion. The sign depends on whether the ambient field possesses mirror symmetry or mirror antisymmetry, defined as follows:

mirror symmetry	mirror antisymmetry
$v_z^\infty(x,y,z) = -v_z^\infty(x,y,-z),$	$v_z^\infty(x,y,z) = v_z^\infty(x,y,-z),$
$v_y^\infty(x,y,z) = v_y^\infty(x,y,-z),$	$v_y^\infty(x,y,z) = -v_y^\infty(x,y,-z),$
$v_x^\infty(x,y,z) = v_x^\infty(x,y,-z);$	$v_x^\infty(x,y,z) = -v_x^\infty(x,y,-z).$

The coefficients can be related as

$$a_{mn}^{(1)} = Sa_{mn}^{(2)}, \quad b_{mn}^{(1)} = Sb_{mn}^{(2)}, \quad c_{mn}^{(1)} = -Sc_{mn}^{(2)},$$

where the superscripts refer to the expansion and with the symmetry parameter S defined by

$$S(\boldsymbol{v}^\infty) = \begin{cases} 1 & \text{if } \boldsymbol{v}^\infty \text{ has mirror symmetry,} \\ -1 & \text{if } \boldsymbol{v}^\infty \text{ has mirror antisymmetry.} \end{cases}$$

The symmetry properties are passed exactly to the collocation approximants if the collocation points on sphere 2 are placed at the mirror images of the points on sphere 1.

We now set the boundary conditions by evaluating the velocity components in the cylindrical coordinate system (z, σ, ϕ). It is then discovered that the ϕ-dependence can be factored as follows. For each boundary-value problem a single term is retained in (3.1), and the value of m for that term is the only one that is required in the velocity representation. After this simplification, one finds that the ϕ-dependence in the z-component and σ-component equations is $\sin m\phi$ for all terms, while for the

ϕ-component of the velocity it is $\cos m\phi$. Thus the ϕ-dependence can be factored to arrive at the following set of equations from the z-, σ- and ϕ-components respectively:

$$\sum_{n=l}^{\infty}\left\{\frac{a_{mn}}{\alpha^2}\left[\frac{n-m+1}{r_1^{n+2}}P_{n+1}^m\xi_1-S\frac{n-m+1}{r_2^{n+2}}P_{n+1}^m(\xi_2)\xi_2\right]\right.$$
$$+b_{mn}\alpha\left[\frac{n(n+1)}{\rho_1}k_n(\rho_1)P_n^m\xi_1+\left(k_n'(\rho_1)+\frac{k_n}{\rho_1}\right)P_n^{m\prime}S_1^2\right.$$
$$\left.-S\frac{n(n+1)}{\rho_2}k_n(\rho_2)P_n^m(\xi_2)\xi_2+\left(k_n'(\rho_2)+\frac{k_n}{\rho_2}\right)P_n^{m\prime}(\xi_2)S_2^2\right]$$
$$\left.+mc_{mn}[k_n(\rho_1)P_n^m-Sk_n(\rho_2)P_n^m(\xi_2)]\right\}$$
$$=A_{lm}[l\xi_1P_l^m+S_1^2P_l^{m\prime}]+B_{lm}mP_l^m, \quad (3.5a)$$

$$\sum_{n=l}^{\infty}\left\{\frac{a_{mn}}{\alpha^2}\left[\frac{n+1}{r_1^{n+2}}P_n^mS_1+\frac{1}{r_1^{n+2}}P_n^{m\prime}S_1\xi_1\right.\right.$$
$$\left.+S\frac{n+1}{r_2^{n+2}}P_n^m(\xi_2)S_2+\frac{S}{r_2^{n+2}}P_n^{m\prime}(\xi_2)S_2\xi_2\right]$$
$$+b_{mn}\alpha\left[\frac{n(n+1)}{\rho_1}k_n(\rho_1)P_n^mS_1-\left(k_n'+\frac{k_n}{\rho_1}\right)P_n^{m\prime}S_1\xi_1\right.$$
$$\left.+S\frac{n(n+1)}{\rho_2}k_n(\rho_2)P_n^m(\xi_2)S_2-S\left(k_n'+\frac{k_n}{\rho_n}\right)P_n^{m\prime}(\xi_2)S_2\xi_2\right]$$
$$\left.-c_{mn}m[k_n(\rho_1)P_n^m\cot\theta_1+Sk_n(\rho_2)P_n^m(\xi_2)\cot\theta_2]\right\}$$
$$=A_{lm}[lS_1P_l^m-\xi_1S_1P_l^{m\prime}]-B_{lm}\frac{m\xi_1}{S_1}P_l^m, \quad (3.5b)$$

$$\sum_{n=l}^{\infty}\left\{-\frac{a_{mn}}{\alpha^2}\left[\frac{m}{r_2^{n+2}}\frac{P_n^m}{S_1}+\frac{Sm}{r_2^{n+2}}\frac{P_n^m(\xi_2)}{S_2}\right]\right.$$
$$+b_{mn}\alpha\left[m\left(k_n'+\frac{k_n}{\rho_1}\right)\frac{P_n^{m\prime}}{S_1}+Sm\left(k_n'+\frac{k_n}{\rho_2}\right)\frac{P_n^{m\prime}(\xi_2)}{S_2}\right]$$
$$\left.+c_{mn}[k_n(\rho_1)P_n^{m\prime}S_1+Sk_n(\rho_2)P_n^{m\prime}(\xi_2)S_2]\right\}$$
$$=A_{lm}\frac{mP_l^m}{S_1}+B_{lm}S_1P_l^{m\prime}, \quad (3.5c)$$

with $\xi_i=\cos\theta_i$, $S_i=\sin\theta_i$ and $\rho_i=\alpha r_i$. P_n^m without an argument denotes $P_n^m(\xi_1)$.

There is an extensive discussion on the optimal location of collocation points in the pioneering work of Gluckman *et al.* (1971). Their principal findings are

(1) equidistant spacing is superior;
(2) the point at the equator is important because it gives the cross-sectional scale;
(3) the system of equations is destabilized if points are placed on the equator;
(4) the system of equations becomes singular if points are placed at the poles.

They circumvented (3) and (4) by using the collocation scheme of figure 3(*b*). The solution was obtained by examining the limit as the twin points approached the

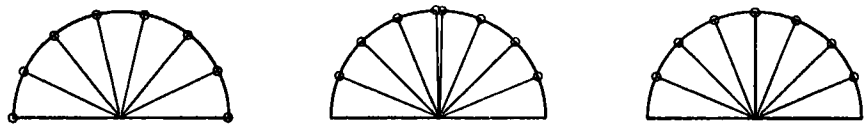

FIGURE 3. Three collocation schemes.

equator (figure 3*c*). For narrow gaps or touching spheres, the cusp geometry at the poles is important. Leichtberg *et al.* (1976) have studied the limiting behaviour as points are placed successively closer to the poles.

Our collocation scheme corresponds to figure 3(*a*). We have observed that if the number of points is 10 or more, placement of a 'point' at the equator is not essential. However, we have discovered a rigorous method for placing points at the poles by removing analytically the singularities from the system of equations and consequently a more robust set of equations at narrow gaps.

The system of equations in (3.5*a*–*c*) becomes singular when a point is placed at a pole, because the z-component equation vanishes (for $m > 0$) and because the σ-component and ϕ-component equations are identical at the poles. The former is due to a zero of multiplicity m, which can be removed by factoring $\sin^m\theta_1$ from the equation. The latter is resolved by examining the difference of (3.5*b*) and (3.5*c*), i.e.

$$\sum_{n=l}^{\infty}\left\{\frac{a_{mn}}{\alpha^2}\left[\frac{n+m}{r_1^{n+2}}P_n^m S_1+\frac{P_n^{m+1}}{r_1^{n+2}}\xi_1+S\ldots\right]\right.$$
$$+b_{mn}\alpha\left[\frac{n(n+1)}{\rho_1}k_n(\rho_1)P_n^m S_1-\left(k_n'+\frac{k_n}{\rho_1}\right)(P_n^{m+1}\xi_1+mP_n^m S_1)+S\ldots\right]$$
$$\left.-c_{mn}[k_n(\rho_1)P_n^{m+1}+Sk_n(\rho_2)P_n^{m+1}(\xi_2)]\right\}$$
$$=A_{lm}[(l-m)S_1P_l^m-\xi_1P_l^{m+1}]-B_{lm}P_l^{m+1}. \quad (3.5d)$$

At the poles it has a zero of multiplicity $m+1$, i.e. it is singular for all problems, which can be removed by factoring $\sin^{m+1}\theta_1$. Thus, if we use (3.5*a*), (3.5*c*) and (3.5*d*) with the zeros removed, including $\sin^{m-1}\theta_1$ from (3.5*c*), then points can be placed at the poles. At the poles the error in the surface velocity resembles an Hermite interpolant, and the cusp geometry is reproduced.

All of the hydrodynamic functions now can be obtained from the coefficients in the velocity expansion. From here on, when we write $a_{mn}(m,l,S)$, $b_{mn}(m,l,S)$ and $c_{mn}(m,l,S)$, the arguments m, l and S indicate that these coefficients were obtained by solving the system of equations (3.5*a*, *c*, *d*) with those parameters. Where necessary, we will specify whether A_{lm} or B_{lm} is used.

3.1. *The drag in a uniform stream*

There are two steps in the determination of $X_F(R;\alpha)$ and $YF(R;\alpha)$. First, l and m are chosen as shown in table 1 and S from the definition for mirror symmetry. Secondly, our expansion is rewritten as a multipole expansion, in gradients of the fundamental solution. The coefficient of the monopole is then identified with X_F and Y_F. After some algebra, we obtain

$$X_F(R;\alpha)=\tfrac{2}{3}a_{01}(0,1,-1), \quad Y_F(R;\alpha)=\tfrac{2}{3}a_{11}(1,1,-1). \quad (3.6a,b)$$

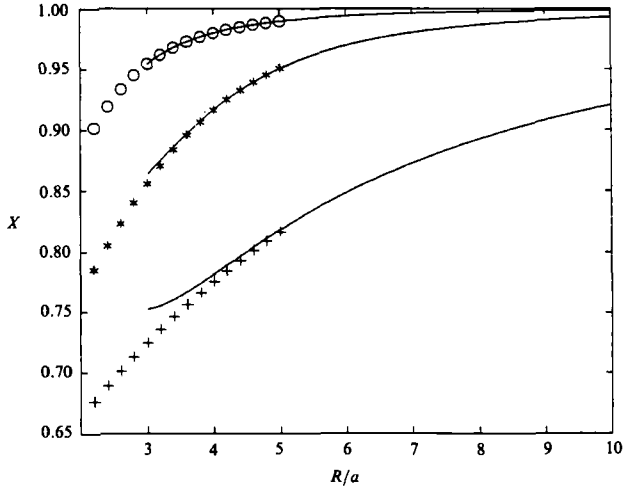

FIGURE 4. Drag on one sphere, normalized by single-sphere result; the sphere–sphere axis is parallel to the uniform stream: +, $\alpha a = 0.1$; *, 1.0; ○, 10.0; ——, method of reflections.

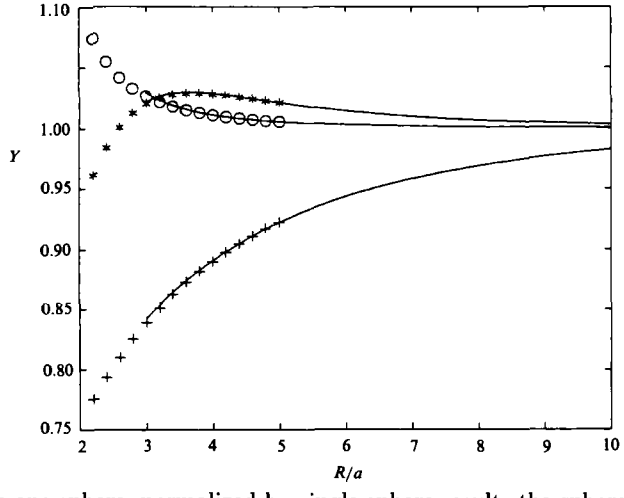

FIGURE 5. Drag on one sphere, normalized by single-sphere result; the sphere–sphere axis is perpendicular to the uniform stream: +, $\alpha a = 0.1$; *, 1.0; ○, 10.0; ——, method of reflections.

with A_{10} and A_{11} non-zero respectively. The plots of these functions (figures 4 and 5), from almost-touching to $R = 5a$, show agreement with the method of reflections. (All plots were obtained with 12-point calculations.)

3.2. *The stresslet in a rate-of-strain field*

The stresslet is determined by the functions $X_S(R;\alpha)$, $Y_S(R;\alpha)$ and $Z_S(R;\alpha)$. Again, l and m are chosen as shown in table 1, S from the definition for mirror symmetry, and the velocity expansion is rewritten as a multipole expansion, in gradients of the fundamental solution. The coefficient of the symmetric dipole is then identified with X_S, Y_S and Z_S. After some algebra, we obtain

$$X_S(R;\alpha) = \tfrac{1}{10}[a_{02}(0,2,1) - R\,a_{02}(0,1,1)], \tag{3.7a}$$

$$Y_S(R;\alpha) = \tfrac{1}{10}[a_{12}(1,2,-1) - \tfrac{3}{2}R\,a_{12}(1,1,-1)], \tag{3.7b}$$

$$Z_S(R;\alpha) = \tfrac{1}{10}a_{22}(2,2,1), \tag{3.7c}$$

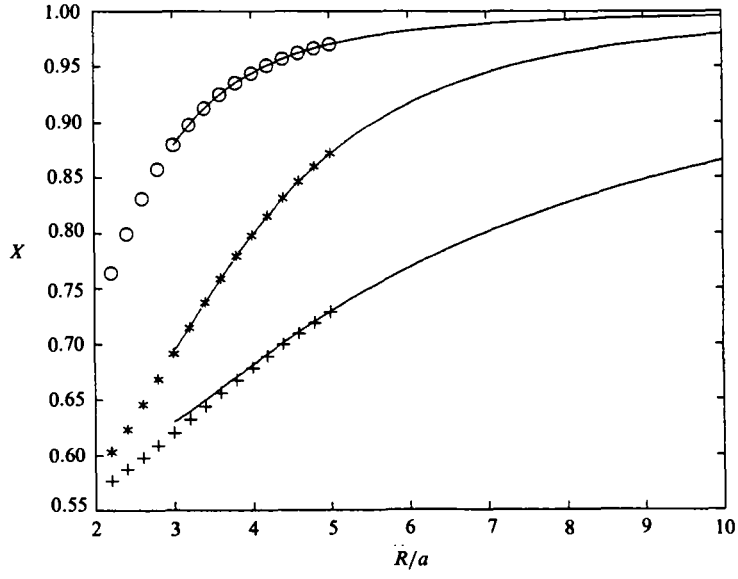

FIGURE 6. Brinkman stresslet function X_S normalized by single-sphere result: +, $\alpha a = 0.1$; *, 1.0; ○, 10.0; ——, method of reflections.

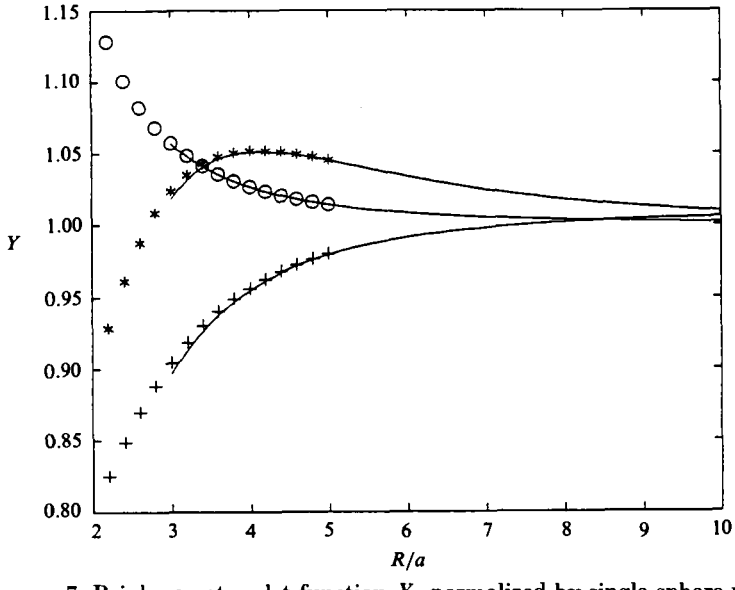

FIGURE 7. Brinkman stresslet function Y_S normalized by single-sphere result: +, $\alpha a = 0.1$; *, 1.0; ○, 10.0; ——, method of reflections.

with the appropriate A_{lm} non-zero. The second terms in (3.7a, b) originate from the translation of the centre of the rate of strain. We have merely exploited the linearity of the Brinkman equation in order to obtain mirror-symmetric problems. Once again, the plots of these functions (figures 6–8), from almost-touching to $R = 5a$, show agreement with the method of reflections.

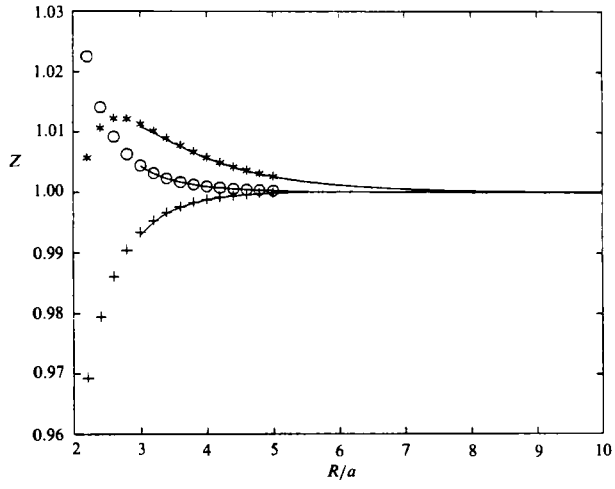

FIGURE 8. Brinkman stresslet function Z_S normalized by single-sphere result: +, $\alpha a = 0.1$; *, 1.0; ○, 10.0; ——, method of reflections.

3.3. *The torque in a vorticity field*

The functions $X_T(R;\alpha)$ and $Y_T(R;\alpha)$ are calculated by choosing l and m as shown in table 1 and S from the definition for mirror symmetry. The velocity expansion is rewritten as a multipole expansion, in gradients of the fundamental solution. The coefficient of the antisymmetric dipole is then identified with X_T and Y_T. After some algebra, we obtain

$$X_T(R;\alpha) = -\tfrac{1}{2}\pi(\alpha a)^{-2}\, c_{01}(0,1,1), \tag{3.8a}$$

$$Y_T(R;\alpha) = -\tfrac{1}{2}\pi(\alpha a)^{-2}\,[c_{11}(1,1,-1) - \tfrac{1}{2}R c_{11}(1,1,1)]. \tag{3.8b}$$

In (3.8a) c_{01} uses $B_{10} = 1$. However, in (3.8b) the first coefficient uses $B_{11} = 1$, while the second uses $A_{11} = 1$. The second term comes from the uniform stream associated with the shift in the centre of the vorticity field. The plots in figures 9 and 10 show the agreement with the method of reflections.

4. Results

The results for the drag functions X_F and Y_F, the stresslet functions X_S, Y_S and Z_S, and the torque functions X_T and Y_T using the collocation technique and the method of reflections are plotted in figures 4–10. All curves have been normalized by the single-sphere result. The behaviour is illustrated for $\alpha a = 0.1$, 1.0 and 10.0. For $R > 3a$, the collocation technique converged to five significant figures with eight collocation points. As expected, agreement between the two methods improved with increasing separation. At a fixed separation the method of reflections gave better results with increasing αa, where the higher-order reflections are damped more rapidly.

We note that for two spheres with their axis perpendicular to the uniform stream (figure 5) the drag exceeds that on an isolated sphere beyond a critical separation. This effect becomes more pronounced with increasing αa, and is due to a transition in the first-reflection contribution. Beyond a screening lengthscale of order α^{-1}, the

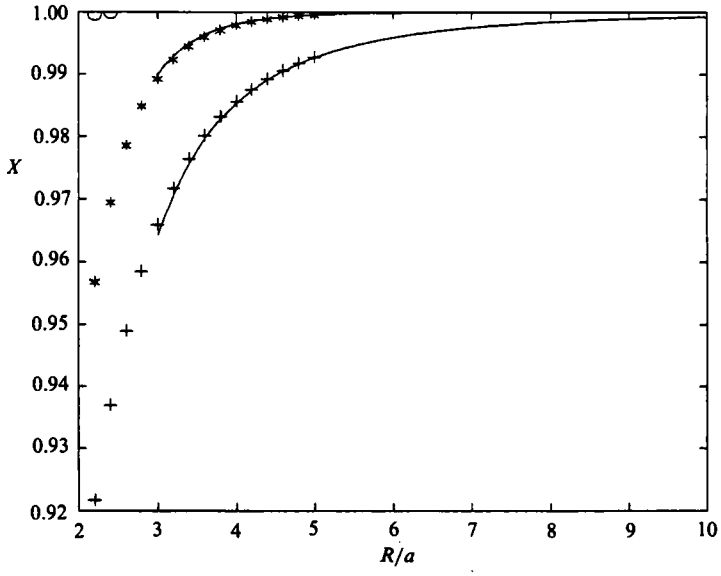

FIGURE 9. Brinkman torque function X_T normalized by single-sphere result: +, $\alpha a = 0.1$; *, 1.0; ○, 10.0; ——, method of reflections.

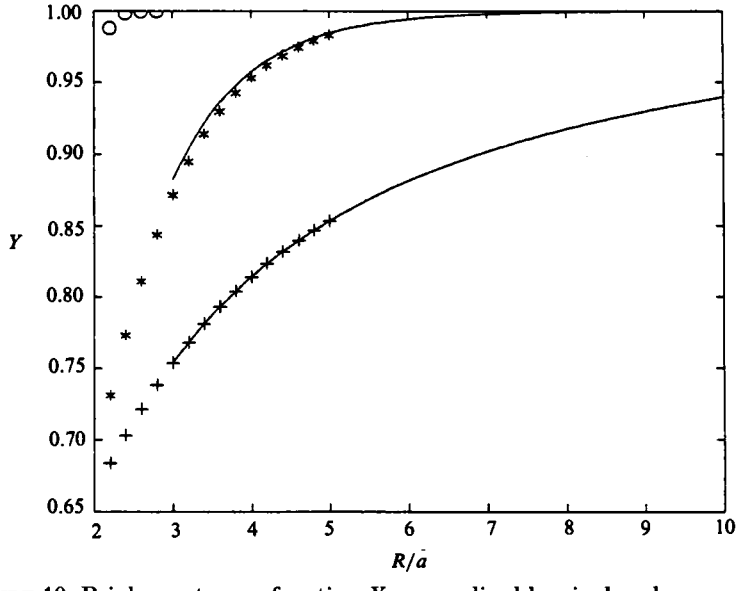

FIGURE 10. Brinkman torque function Y_T normalized by single-sphere result: +, $\alpha a = 0.1$; *, 1.0; ○, 10.0; ——, method of reflections.

streamlines of the fundamental solution of the Brinkman equation resemble a dipole field, and the flow is opposite to the direction of the point force (as in the fieldlines for a magnetic dipole). Thus, if the second sphere lies beyond the screening lengthscale, the first reflection increases the drag on the first sphere. For $\alpha = O(1)$, Y_F has a readily distinguished maximum because the contribution from the first

reflection reverts to the usual behaviour in the near field. This effect is also present in Y_S and Z_S.

For the stresslet and torque functions, at fixed values of αa, R and number of collocation points, the agreement between the method of reflections and the collocation solution is superior for the Z_S and X_T functions. This arises because the dominant contributions to the stresslet and torque, i.e. the ones that trace back to the monopole field induced by the sphere at x_2, contain no Z_S and X_T components. Thus the hydrodynamic interactions decay more rapidly for these functions.

This material is based upon work supported by the National Science Foundation under grant CPE-8116339 to W.B.R. Additional funding was provided by the Westvaco Corporation and the George Van Ness Lothrop Fellowship to S.K. from the School of Engineering, Princeton University.

REFERENCES

Abramowitz, M. & Stegun, I. 1964 *Handbook of Mathematical Functions*. National Bureau of Standards.

Batchelor, G. K. & Green, J. T. 1972 *J. Fluid Mech.* **56**, 375.

Brenner, H. 1972 *Chem. Engng Sci.* **27**, 1069.

Brinkman, H. C. 1947 *Appl. Sci. Res.* **A1**, 27.

Faxen, H. 1922 *Ark. Mat. Astron. Fys.* **17**, no. 1.

Faxen, H. 1927 *Ark. Mat. Astron. Fys.* **20**, no. 8.

Felderhof, B. U. 1975 *Physica* **80A**, 63, 172.

Felderhof, B. U. & Deutch, J. M. 1975 *J. Chem. Phys.* **62**, 2879, 2398.

Ganatos, P., Pfeffer, R. & Weinbaum, S. 1978 *J. Fluid Mech.* **84**, 79.

Ganatos, P., Pfeffer, R. & Weinbaum, S. 1980 *J. Fluid Mech.* **99**, 755.

Glendinning, A. B. & Russel, W. B. 1983 *J. Coll. Interface Sci.* **93**, 95.

Gluckman, M. J., Pfeffer, R. & Weinbaum, S. 1971 *J. Fluid Mech.* **50**, 705.

Goldman, A. J., Cox, R. G. & Brenner, H. 1966 *Chem. Engng Sci.* **21**, 1151.

Happel, J. & Brenner, H. 1965 *Low Reynolds Number Hydrodynamics*. Prentice-Hall.

Higdon, J. J. L. & Kojima, M. 1981 *Intl J. Multiphase Flow* **7**, 719.

Hobson, E. 1955 *The Theory of Spherical and Ellipsoidal Harmonics*. Chelsea.

Howells, I. D. 1974 *J. Fluid Mech.* **64**, 449.

Kim, S. & Russel, W. B. 1985 *J. Fluid Mech.* **154**, 269.

Koplik, J., Levine, H. & Zee, A. 1983 *Phys. Fluids* **26**, 2864.

Leichtberg, S., Weinbaum, S., Pfeffer, R. & Gluckman, M. J. 1976 *Phil. Trans. R. Soc. Lond.* A **282**, 585.

Stimson, M. & Jeffery, G. B. 1926 *Proc. R. Soc. Lond.* A **111**, 110.

Stratton, J. A. 1941 *Electromagnetic Theory*. McGraw-Hill.